

## SPECTROPHOTOMETRIC DETERMINATION OF REACTION STOICHIOMETRY AND EQUILIBRIUM CONSTANTS OF METALLOCHROMIC INDICATORS. II. THE $\text{Ca}^{2+}$ –ARSENAZO III COMPLEXES

Peter L. DOROGI and Eberhard NEUMANN

*Max-Planck-Institut für Biochemie, D-8033 Martinsried, Munich, FRG*

Received 15 July 1980

The analytical method described in the preceding article was applied to spectrophotometric  $\text{Ca}^{2+}$ -titrations of the metallochromic indicator arsenazo III (Ar). At various reactant concentrations it was determined that Ar forms 1 : 1, 1 : 2 and 2 : 1 complexes with calcium. The equilibrium constants and extinction coefficients at 602 nm were determined. Corrected to zero ionic strength at 293 K and pH 7.0, the reactions  $\text{Ca} + \text{Ar} = \text{CaAr}$ ,  $\text{CaAr} + \text{Ar} = \text{CaAr}_2$  and  $\text{CaAr} + \text{Ca} = \text{Ca}_2\text{Ar}$  are associated with dissociation equilibrium constants  $K_{11} = 1.6 \times 10^{-6} \text{ M}$ ,  $K_{12} = 3.2 \times 10^{-4} \text{ M}$  and  $K_{21} = 5.8 \times 10^{-3} \text{ M}$ , respectively. The extinction coefficient of unbound indicator is  $\epsilon_{602} = 9.6 (\pm 0.3) \times 10^3 \text{ cm}^{-1} \text{ M}^{-1}$ . Arsenazo III complexes with monovalent ions like  $\text{Na}^+$  and  $\text{K}^+$ : at zero ionic strength, the dissociation constant of the  $\text{Na}^+$ –Ar complex is about 0.1 M.

### 1. Introduction

The metallochromic indicator arsenazo III (2,7-bis-(2-arsonophenylazo)-1,8-dihydroxynaphthalene-3,6-disulfonic acid) has been used extensively as a  $\text{Ca}^{2+}$  indicator in a variety of physiological preparations. For example, it has been applied to the measurement of  $\text{Ca}^{2+}$ -efflux from liposomes [1],  $\text{Ca}^{2+}$ -transport in sarcoplasmic reticulum [2] and to the determination of intra-cellular  $\text{Ca}^{2+}$  levels [3]. Upon complexing with  $\text{Ca}^{2+}$ , the absorbance maximum of arsenazo III shifts in the visible range from a wavelength of 560 nm to maxima at 602 and 660 nm (shifting the color from red to blue); the difference in molar extinction coefficient between  $\text{Ca}^{2+}$ -free and  $\text{Ca}^{2+}$ -bound indicator is large, on the order of  $10^4 \text{ cm}^{-1} \text{ M}^{-1}$  [4].

The major advantage of arsenazo III over other commonly used calcium indicators is the high binding affinity, allowing application at very low calcium concentrations. Disadvantages include the relatively poor selectivity for  $\text{Ca}^{2+}$ , resulting in interference from  $\text{Mg}^{2+}$  and monovalent cations, and the relatively slow rate of complexing, which interferes with time resolution of rapid kinetic events [5].

A satisfactory theoretical characterization of the  $\text{Ca}^{2+}$ –arsenazo III interaction has not yet been achieved,

because all the binding parameters can not be determined from conventional double reciprocal plots (e.g., as done in ref. [6]). It has been observed that the absorbance changes are no longer linear functions of calcium concentration when calcium concentration is raised above 10  $\mu\text{M}$  [5], suggesting that the indicator forms higher-order complexes with calcium. The presence of indicator dimers in the presence of  $\text{Ca}^{2+}$  has been suggested [7]. Calcium–arsenazo III interaction appears complicated, and since at physiological calcium concentrations an appreciable amount of  $\text{Ca}^{2+}$  would be bound to the indicator, a complete description of this complicated interaction is necessary for accurate determinations of free  $\text{Ca}^{2+}$  levels in biological systems. It will become apparent that standard binding analyses are inadequate to calibrate arsenazo III, except in concentration ranges where the interaction with metal ions is limited to only one type of complex.

Application of the new method, outlined in Part I of this series, clearly indicates that during a spectrophotometric titration with  $\text{Ca}^{2+}$  three types of complexes are formed. The prevailing stoichiometries are determined by the concentrations of the reactants. The method also resolves small differences between the extinction coefficients of the three complexes: these differences can be important if arsenazo III is used as an

indicator of  $\text{Ca}^{2+}$  binding properties in calcium concentration ranges where most of the indicator is in the bound form.

## 2. Materials and methods

Since commercial arsenazo III (obtained from Aldrich, Milwaukee) is thin-layer chromatographically a multi-component mixture, the raw material has been purified according to the methods described by Kendrick [8]. In brief, 450 mg of arsenazo III (acid) is suspended in 2 ml  $\text{H}_2\text{O}$ , and a few droplets of 1N NaOH are added to dissolve the dye; 3 ml of Solution I are then added. Solution I contains n-butanol, pyridine, acetic acid and  $\text{H}_2\text{O}$ , according to the volume ratio 3 : 1 : 1 : 3; pH 4.7. The dye solution is applied to a  $2.5 \times 35$  cm column filled with pre-swollen DEAE-cellulose (Whatman DE52) which has been suspended in Solution I. The last of at least five differently colored fractions is dark violet and contains the Na-salt of arsenazo III. This fraction is repeatedly evaporated under addition of  $\text{H}_2\text{O}$  to eliminate the pyridine, using a vacuum rotatory evaporator. The dry dye was dissolved in 50 ml  $\text{H}_2\text{O}$  and passed through an ion-exchange column ( $1.5 \times 20$  cm) filled with the Na-form of Chelex 100 (100–400 mesh, Biorad Lab.) to remove traces of  $\text{Ca}^{2+}$ . The eluate is reduced in volume under vacuum and lyophilized. The approximately 250 mg of dry amorphous powder is dissolved in 5 ml  $\text{H}_2\text{O}$  and concentrated HCl is added to yield a final concentration of 6 M HCl. Under cold conditions ( $4^\circ\text{C}$  for 12 h) the dye precipitates; it is then collected by filtration and vacuum dried. The yield was 180 mg of chromatographically pure arsenazo III ( $R_f = 0.18$ ). By atomic absorption spectroscopy, this purified sample contains 0.008 mole  $\text{Ca}^{2+}$  and 0.4 mole  $\text{Na}^+$  per mole of arsenazo III. Ion exchange using Chelex 100 and acid precipitation are alone not sufficient to purify the dye: the analysis of spectrophotometric titrations leads to erroneous results [9].

All chemicals used were of grade Suprapur, Merck. Deionized water was quartz-reflux distilled, with a conductivity of  $0.9 \mu\text{S cm}^{-1}$  at 293 K. All vessels were washed with 1  $\mu\text{M}$  EDTA-solution and then rinsed with distilled water; wherever possible, plastic vessels were used.

The  $\text{Ca}^{2+}$  content of the purified dye and buffer

used in the spectrophotometric titrations were determined by atomic absorption spectroscopy. Titrations were performed at 293 K in a thermostated cell with the Cary 118 spectrometer. The sample cell was equipped with a magnetic stirring device, and the initial sample volume was 2.4 ml. The dye was dissolved in 0.03 M N-hydroxyethylene-piperazine-N'-ethylene-sulfonic acid (Pipes, pH 7.0) and the final pH was always adjusted to 7.0; the final ionic strength was 0.03 M. Under these conditions, where  $[\text{Na}^+] = 0.03$  M, the contribution of  $\text{Na}^+$ -indicator complexes to the absorbance is negligibly small.

## 3. Optical and thermodynamic constants

### 3.1. Extinction coefficient of unbound arsenazo III

Accurate determination of the extinction coefficient of free arsenazo III can be seriously hampered by cation contamination from both buffer and indicator salts, but this contamination is expected to be unimportant if total indicator ( $[\text{Ar}_T]$ ) and salt concentrations are sufficiently reduced. (Throughout this article we will use the symbols and notation defined in the preceding article [10], henceforth referred to with the Roman numeral I.) According to eq. (9) of I, the extinction coefficient of free arsenazo III,  $\epsilon_{\text{Ar}}$ , may be estimated from the zero concentration limit of the total absorbance  $A$ , per cm,

$$\epsilon_{\text{Ar},602} = \lim_{[\text{Ar}_T] \rightarrow 0} A_{602}/[\text{Ar}_T], \quad (1)$$

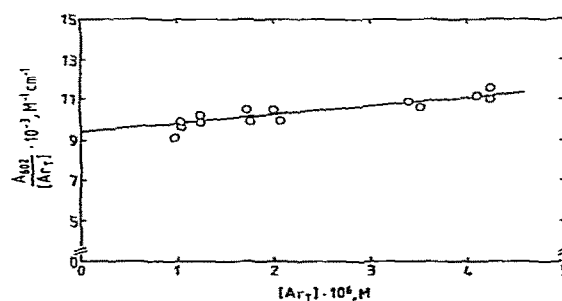


Fig. 1. Graphical estimation of  $\epsilon_{\text{Ar}}$  using eq. (1). Progressive dilution indicates  $\epsilon_{\text{Ar}} = 9.6(\pm 0.3) \times 10^3 \text{ cm}^{-1} \text{ M}^{-1}$  at  $I_c = 0.03$  M, pH 7.0, 293 K.

the subscripts indicate that all absorbance measurements, including the spectrophotometric  $\text{Ca}^{2+}$  titrations, were done at  $\lambda = 602$  nm, where the  $\text{Ca}^{2+}$ -specific absorbance changes are maximal. The graphical extrapolation procedure suggested by eq. (1) could be easily performed in the present case, because the ratio  $A_{602}/[\text{Ar}_T]$  varied practically linearly with  $[\text{Ar}_T]$ . The result is shown in fig. 1; at ionic strength  $I_c = 0.03$  M, pH 7.0 and temperature  $T = 293$  K, we obtain  $\epsilon_{\text{Ar}} = 9.6 (\pm 0.3) \times 10^3 \text{ cm}^{-1} \text{ M}^{-1}$  at 602 nm, within the scatter of experimental points.

### 3.2. Calcium binding constants and optical parameters

Indicator solutions characterized by nine different arsenazo III concentrations were titrated with concentrated  $\text{CaCl}_2$  plus buffer solutions. For graphical data representation, and for the visual detection of the saturation level at high  $\text{Ca}^{2+}$  concentrations, it is useful to refer changes in absorbance ( $\Delta A$ ) to the initial total concentration of indicator,  $[\text{Ar}_T]_0$ , at the initial volume  $v_0$  at the start of the titration:

$$\Delta A_0 = A \frac{v}{v_0} - \epsilon_{\text{Ar}} [\text{Ar}_T]_0; \quad (2)$$

$v$  is the total volume of the solution after adding increments of  $\text{CaCl}_2$ -buffer solution.

Five spectrophotometric titration curves are shown in fig. 2. No simple graphical procedure (e.g. double

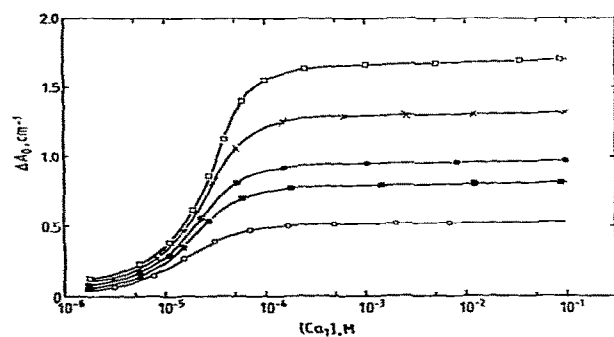


Fig. 2. Absorbance changes at 602 nm,  $\Delta A_0$ , related to the initial value,  $\epsilon_{\text{Ar}} [\text{Ar}_T]_0$ , for  $[\text{Ar}_T] = 1.604 \times 10^{-5}$  M (open circles),  $2.512 \times 10^{-5}$  M (solid squares),  $3.000 \times 10^{-5}$  M (solid circles),  $3.988 \times 10^{-5}$  M (crosses) and  $5.204 \times 10^{-5}$  M (open squares); pH 7.0, 293 K.

reciprocal plot of  $\Delta A_0$  versus  $[\text{Ca}]$ ) can satisfactorily analyze the data in terms of equilibrium binding and optical constants. This finding suggested that the calcium-arsenazo III interaction is complicated and the analytical method described in I was applied. In brief,  $[\text{Ca}_T]$  and  $[\text{Ar}_T]$  must be first chosen such that only the stoichiometrically simplest complex contributing to  $\Delta A$  is appreciable, allowing approximate determination of its parameters. Higher-order complexes can be characterized subsequently by increasing  $[\text{Ca}_T]$  and/or  $[\text{Ar}_T]$ .

At first,  $\Delta A$  is assumed to be a reflection of the overall complexation reaction



with overall dissociation equilibrium constant  $K'_{pq}$ , defined by

$$K'_{pq} = \frac{[\text{Ca}]^p [\text{Ar}]^q}{[\text{Ca}_p\text{Ar}_q]} \quad (4)$$

$$= \frac{\{[\text{Ca}_T] - p\Delta A/(q\Delta\epsilon_{pq})\}^p \{[\text{Ar}_T] - \Delta A/\Delta\epsilon_{pq}\}^q}{\Delta A/(q\Delta\epsilon_{pq})}$$

the subscript zero has been dropped from  $\Delta A$  to simplify notation, and  $\Delta\epsilon_{pq}$  denotes the change in molar absorptivity of the indicator due to  $\text{Ca}_p\text{Ar}_q$  complexation (c.f. eq. (7) of I).

The simplest complex formed must be  $\text{CaAr}$ : for this case  $p = q = 1$ , and the overall constant  $K'_{11}$  is the elementary equilibrium constant  $K_{11}$ . The 1 : 1 complex would dominate at low concentrations, where the free indicator-bound indicator equilibrium lies toward the free form. Therefore, if  $\text{CaAr}$  contributes to the optical signal at all, its properties will be most easily resolvable from the experimental points with the lowest  $[\text{Ar}_T]$  and  $[\text{Ca}_T]$  values. The test criterion for resolution of the 1 : 1 complex is that the rhs of eq. (4) remain at the same numerical value as the various data points ( $\Delta A$ ,  $[\text{Ca}_T]$ ,  $[\text{Ar}_T]$ ) are inserted. If a value of  $\Delta\epsilon_{11}$  can be found which satisfies this constancy condition, then the value of  $K_{11}$  is at the same time determined.

Although for the titration curves corresponding to higher  $[\text{Ar}_T]$  no satisfactory  $\Delta\epsilon_{11}$  value could be resolved, low  $[\text{Ar}_T]$  curves could show constancy at low  $[\text{Ca}_T]$  values, which suggested that these curves have regions wherein  $\text{CaAr}$  complexation is largely responsible for  $\Delta A$ . It is important to note that no integer choice for  $p$  and  $q$ , except  $p = q = 1$ , yielded a constant  $K'_{pq}$

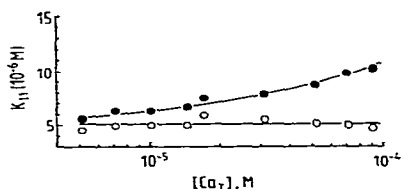


Fig. 3. Equilibrium constant for the  $\text{CaAr}$  complex,  $K_{11}$ , as a function of total calcium concentration,  $[\text{Ca}_T]$  (eq. (4)): open circles are for  $\Delta\epsilon_{11} = 3.2 \times 10^4 \text{ cm}^{-1} \text{ M}^{-1}$  (optimum values), while solid circles show, for example, that calculation with  $\Delta\epsilon_{11} = 3.4 \times 10^4 \text{ cm}^{-1} \text{ M}^{-1}$  is unsatisfactory.

for any of the titration curves. As argued above, the absence of constant- $K'_{pq}$  regions for the higher  $[\text{Ar}_T]$  curves indicates mixing of different stoichiometric types.

Fig. 3 shows one  $K_{11}$ -curve, corresponding to a titration with  $[\text{Ar}_T] = 1.60 \times 10^{-5} \text{ M}$ . Plotted  $K_{11}$  values have been adjusted for differences in total ionic strength as  $[\text{Ca}_T]$  is varied, as described in I, using the valence model



Although at pH 7.0 each arsenazo III molecule is expected to have a charge number  $-5$ , the *effective* charge number at the  $\text{Ca}^{2+}$  binding site for activity coefficient corrections is expectedly reduced due to spatial separation of charges on the molecule, i.e., the arsenazo III molecule is not expected to behave like a point charge. The effective charge number of  $-3$  was determined to be optimum for "fine" fitting of the overall reaction model, to be described below.  $K_{11}$  values shown in fig. 3 refer to the buffer ionic strength 0.03 M, and illustrate the prediction of eq. (4) for low  $[\text{Ca}_T]$  values when  $\Delta\epsilon_{11}$  is set at  $3.4 \times 10^4 \text{ cm}^{-1} \text{ M}^{-1}$  and at  $3.2 \times 10^4 \text{ cm}^{-1} \text{ M}^{-1}$ .  $\Delta\epsilon_{11} = 3.2 \times 10^4 \text{ cm}^{-1} \text{ M}^{-1}$  proved to be the optimum value and it could be estimated that  $K_{11} \approx 6.4 \times 10^{-6} \text{ M}$ . As  $[\text{Ca}_T]$  increases (not shown in fig. 3), the trend of calculated  $K_{11}$  values deviates markedly from horizontal behavior, indicating that reaction (5) cannot cover the experimental data at higher  $[\text{Ca}_T]$  values.

As noted above, for higher  $[\text{Ar}_T]$  no integer choice of  $p$  and  $q$  gave satisfactory results, even at low  $[\text{Ca}_T]$  values. It is therefore expected that *at least* one other reaction becomes important as  $[\text{Ar}_T]$  is raised; the likely candidate is



This reaction may be stabilized, for example, if the  $\text{CaAr}_2$  configuration affords a more favorable chelating environment for  $\text{Ca}^{2+}$  ions than does the aqueous hydration shell. As described in I, the dissociation equilibrium constant of this reaction,  $K_{12}$ , and the *average* extinction coefficient of Ar molecules in the complex  $\text{CaAr}_2$ ,  $\Delta\epsilon_{12}$ , can be evaluated if  $K_{11}$  and  $\Delta\epsilon_{11}$  are known:

$$K_{12} = \frac{[\text{CaAr}][\text{Ar}]}{[\text{CaAr}_2]} = \frac{2\Delta\epsilon_{12}[\text{Ca}][\text{Ar}]^2}{\Delta A K_{11} - [\text{Ca}][\text{Ar}]\Delta\epsilon_{11}} \quad (7)$$

As shown in I, both  $[\text{Ca}]$  and  $[\text{Ar}]$ , and hence  $K_{12}$ , can be reduced to functions of only one unknown,  $\Delta\epsilon_{12}$ . The test for resolution of  $\Delta\epsilon_{12}$  is based on the constancy condition for  $K_{12}$  (eq. (7)), which then also *determines*  $K_{12}$ . It is noteworthy that eq. (7) depends not only on  $\Delta\epsilon_{12}$ , but also on  $K_{11}$  and  $\Delta\epsilon_{11}$ ; therefore, this step in the analysis is a critical measure of these parameters as well. A constant value for  $K_{12}$  will assumedly result *only if* the measured  $\Delta A$  values are indeed principally due to  $\text{CaAr}$  and  $\text{CaAr}_2$ , and if one has inserted the correct values for  $K_{11}$ ,  $\Delta\epsilon_{11}$  and  $\Delta\epsilon_{12}$ . If one is measuring in concentration ranges wherein  $\Delta A$  reflects  $\text{CaAr}$  to a larger extent than  $\text{CaAr}_2$ , then inaccuracies in the measured quantities ( $\Delta A$ ,  $[\text{Ar}_T]$ ,  $[\text{Ca}_T]$ ) will result in large scatter for calculated values of  $K_{12}$ : this increased scatter reflects the higher sensitivity needed to resolve the  $\text{CaAr}_2$  contribution to  $\Delta A$  when  $\text{CaAr}$  dominates.

The desired horizontal  $K_{12} - [\text{Ca}_T]$  curve was obtained for *all*  $[\text{Ar}_T]$  values for low  $[\text{Ca}_T]$ , i.e., test condition eq. (7) could be satisfied of all  $[\text{Ar}_T]$  conditions whereas the 1 : 1 model (eq. (4) with  $p = q = 1$ ) could not. Two cases, with  $[\text{Ar}_T] = 4.782 \times 10^{-5} \text{ M}$  and  $5.204 \times 10^{-5} \text{ M}$ , are shown in fig. 4.  $K_{11}$  had to be raised above the value suggested in fig. 3, to  $1.1 \times 10^{-5} \text{ M}$ , suggesting that  $[\text{Ar}_T]$  values would have to be lowered further before a pure 1 : 1 stoichiometric model would be actually adequate. Extensive trial-and-error calculations, varying  $K_{11}$ ,  $\Delta\epsilon_{11}$  and  $\Delta\epsilon_{12}$  over wide ranges, showed that the desired constancy in  $K_{12}$  is reproduced *only* with the choice of parameters

$$K_{11} = 1.1 \times 10^{-5} \text{ M}, \quad \Delta\epsilon_{11} = 3.2 \times 10^4 \text{ cm}^{-1} \text{ M}^{-1},$$

$$\text{and } \Delta\epsilon_{12} = 3.3 \times 10^4 \text{ cm}^{-1} \text{ M}^{-1}.$$

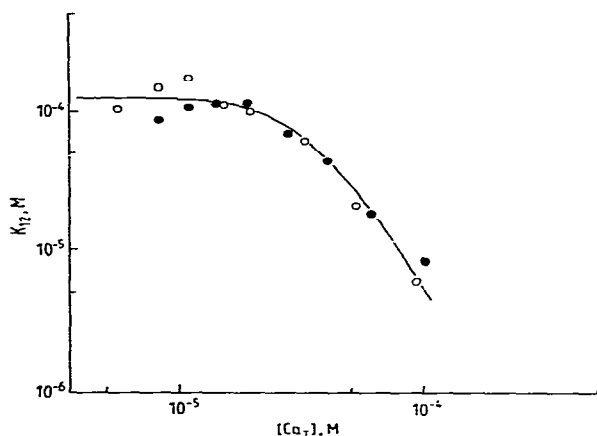
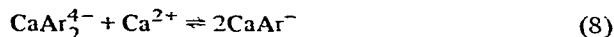


Fig. 4. Equilibrium constant,  $K_{12}$  (eq. (7)), for two titrations:  $[\text{Ar}_T] = 5.204 \times 10^{-5} \text{ M}$  (solid circles) and  $4.782 \times 10^{-5}$  (open circles), as a function of total calcium concentration. Parameters are  $K_{11} = 1.1 \times 10^{-5} \text{ M}$ ,  $\Delta\epsilon_{11} = 3.2 \times 10^4 \text{ cm}^{-1} \text{ M}^{-1}$  and  $\Delta\epsilon_{12} = 3.3 \times 10^4 \text{ cm}^{-1} \text{ M}^{-1}$ ;  $K_{12}$  is estimated as about  $1.2 \times 10^{-4} \text{ M}$  at ionic strength 0.03 M.

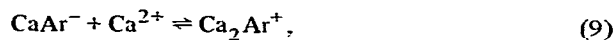
The range of predicted  $K_{12}$  values for the entire set of nine titration curves was between  $1.0 \times 10^{-4} \text{ M}$  and  $1.4 \times 10^{-4} \text{ M}$ .

The large deviation from horizontal for  $[\text{Ca}_T] > 2 \times 10^{-5} \text{ M}$  in fig. 4, does not necessarily mean that a third type of complex, other than  $\text{CaAr}$  and  $\text{CaAr}_2$ , is prevalent. Rather, the observed nonhorizontal trend can reflect the gradual disappearance of the  $\text{CaAr}_2$  complex via the disproportionation reaction



as  $[\text{Ca}_T]$  is raised. As discussed above, resolution of  $K_{12}$  becomes progressively more difficult and unreliable as the relative contribution of  $\text{CaAr}_2$  to  $\Delta A$  diminishes. On the other hand, a test equivalent to that shown in fig. 3, with  $p = q = 1$ , but now applied to the high  $[\text{Ca}_T]$  ranges, showed that the complex  $\text{CaAr}$  does not cover  $\Delta A$  at high  $[\text{Ca}_T]$ : at least one additional type of complex becomes important at high  $[\text{Ca}_T]$ .

The immediate choice for the third complex is  $\text{Ca}_2\text{Ar}$ . As before, a constancy test can be used to check the validity of this assumption. The dissociation constant for the reaction



$K_{21}$ , was estimated using the three-complex formalism of I, which incorporates  $K_{11}$ ,  $K_{12}$ ,  $\Delta\epsilon_{11}$  and  $\Delta\epsilon_{12}$  as known parameters (Actually, given the apparent disappearance of  $\text{CaAr}_2$  at high  $[\text{Ca}_T]$  values, the two-complex formalism treating  $\text{CaAr}$  and  $\text{Ca}_2\text{Ar}$  could have been used, but the formalism incorporating  $\text{CaAr}_2$  is expectedly more sensitive at low reactant concentrations.) As described in I, in the presence of  $\text{CaAr}$ ,  $\text{CaAr}_2$  and  $\text{Ca}_2\text{Ar}$  the expression for  $\Delta A$  may be written in the form

$$\begin{aligned} \Delta A = & (\Delta\epsilon_{11} - \Delta\epsilon_{21}/2)[\text{Ca}][\text{Ar}]/K_{11} \\ & + (2\Delta\epsilon_{12} - \Delta\epsilon_{21}/2)[\text{Ca}][\text{Ar}]^2/(K_{11}K_{12}) \\ & + (\Delta\epsilon_{21}/2)([\text{Ca}_T] - [\text{Ca}]). \end{aligned} \quad (10)$$

Both  $[\text{Ca}]$  and  $K_{21}$  can be expressed in terms of one unknown,  $[\text{Ar}]$  (c.f. eqs. (29) and (31) of I); for each choice of  $\Delta\epsilon_{21}$ , the value of  $[\text{Ar}]$  was found which satisfied eq. (10), and the corresponding value of  $K_{21}$  was also calculated. The procedure was repeated until a value of  $\Delta\epsilon_{21}$  was found which gave a horizontal  $K_{21}-[\text{Ca}_T]$  curve at high  $[\text{Ca}_T]$  values. This test criterion can be satisfied only in concentration ranges where  $\text{Ca}_2\text{Ar}$  makes a substantial contribution to  $\Delta A$ ; results for one titration curve, with  $[\text{Ar}_T] = 4.782 \times 10^{-5} \text{ M}$ , are shown in fig. 5, with  $\Delta\epsilon_{21}$  set at the optimum value,  $\Delta\epsilon_{21} = 3.45 \times 10^4 \text{ cm}^{-1} \text{ M}^{-1}$ .  $K_{21}$  can be judged to be about

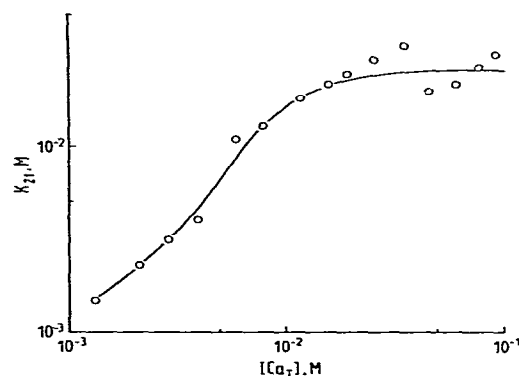


Fig. 5. Equilibrium constant,  $K_{21}$ , from a single titration,  $[\text{Ar}_T] = 4.782 \times 10^{-5} \text{ M}$  as a function of total calcium concentration, using eq. (31) of I; Parameters were  $K_{11} = 1.1 \times 10^{-5} \text{ M}$ ,  $K_{12} = 1.2 \times 10^{-4} \text{ M}$ ,  $\Delta\epsilon_{11} = 3.2 \times 10^4 \text{ cm}^{-1} \text{ M}^{-1}$ ,  $\Delta\epsilon_{12} = 3.3 \times 10^4 \text{ cm}^{-1} \text{ M}^{-1}$  and  $\Delta\epsilon_{21} = 3.45 \times 10^4 \text{ cm}^{-1} \text{ M}^{-1}$ ;  $K_{21}$  is estimated as  $2.5 \times 10^{-2} \text{ M}$ .

Table I

Thermodynamic and optical constants per mole of indicator characterizing the arsenazo III–Ca<sup>2+</sup> interactions at pH 7.0 and 293 K and various ionic strengths,  $I_c$ ; see text

Reaction	$K_{pq}$ (M)	$I_c = 0$	$I_c = 0.01$ M	$I_c = 0.1$ M	$\Delta\epsilon_{pq}$ (cm <sup>-1</sup> M <sup>-1</sup> )
Ca + Ar = CaAr	$K_{11}$	$1.6 \times 10^{-6}$	$5.4 \times 10^{-6}$	$3.0 \times 10^{-5}$	$\Delta\epsilon_{11} = 3.2 \times 10^4$
CaAr + Ar = CaAr <sub>2</sub>	$K_{12}$	$3.2 \times 10^{-4}$	$1.7 \times 10^{-4}$	$6.9 \times 10^{-5}$	$\Delta\epsilon_{12} = 3.3 \times 10^4$
CaAr + Ca = Ca <sub>2</sub> Ar	$K_{21}$	$5.8 \times 10^{-3}$	$8.7 \times 10^{-3}$	$1.5 \times 10^{-2}$	$\Delta\epsilon_{21} = 3.45 \times 10^4$

$2.5 \times 10^{-2}$  M; this result was found for all titration curves. A listing of all size binding and optical parameters is given in table I.

The entire set of results were checked for consistency by recalculating  $\Delta A$  from the expression

$$\Delta A = \Delta\epsilon_{11} [\text{CaAr}] + 2\Delta\epsilon_{12} [\text{CaAr}_2] + \Delta\epsilon_{21} [\text{Ca}_2\text{Ar}], \quad (11)$$

the concentrations appearing in eq. (11) were calculated from the determined values of  $K_{11}$ ,  $K_{12}$  and  $K_{21}$  for each titration point. Using the values given in table I (corrected to  $I_c = 0.03$  M), the calculated  $\Delta A$  curves came within 2% of the measured  $\Delta A$  while satisfying mass conservation requirements to within 1% of  $[\text{Ca}_T]$  and  $[\text{Ar}_T]$  for each titration point. The calculated distribution of calcium–arsenazo III complexes for  $[\text{Ar}_T] = 4.728 \times 10^{-5}$  M is shown in fig. 6.

#### 4. Discussion

The analytical technique applied to the determina-

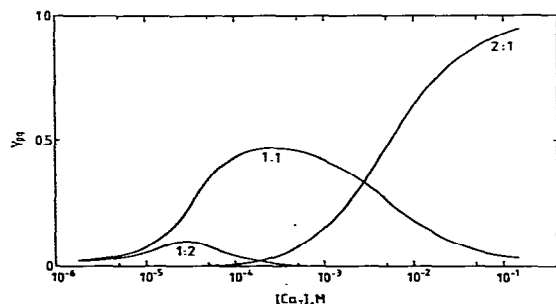


Fig. 6. Fraction of indicator bound,  $\gamma_{pq}$ , in the three individual complexes when  $[\text{Ar}_T] = 4.782 \times 10^{-5}$  M;  $\gamma_{pq} = q[\text{Ca}_p\text{Ar}_q]/[\text{Ar}_T]$ ; see text.

tion of thermodynamic and optical parameters of the Ca<sup>2+</sup>–arsenazo III complexes is limited only by the accuracy of experimentally determined quantities. Metal ion and indicator concentrations may be selected so as to favor a particular complex, and thereby provide reliable estimates of stoichiometry, equilibrium constant and extinction coefficient. In fact, it is the high sensitivity of the constancy tests which renders the method very effective: sensitivity is high to the choices for  $p$ ,  $q$  and  $\Delta\epsilon_{pq}$ , with estimates of  $K_{pq}$  being somewhat less accurate.

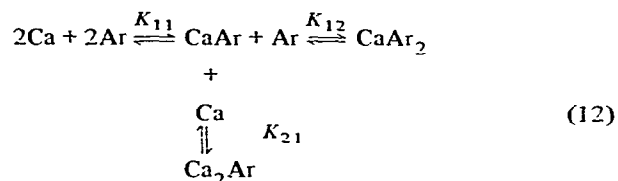
Proper choice for the charge number of arsenazo III in the activity coefficient corrections was judged to be  $-3$ : this was the optimum value for fine fitting high  $[\text{Ca}_T]$  points on the titration curves, where these corrections are the most crucial.

In view of the controversial *ad hoc* assumptions on stoichiometry [2,6], the most important result of this study is that arsenazo III forms at least three different types of individual complexes with Ca<sup>2+</sup> ions. The extinction coefficients per mole of indicator are, however, not very different.

The absorbance relaxation spectrum of the Ca<sup>2+</sup>–arsenazo III system displays three distinct relaxation modes, in agreement with the reaction complexity found here; the time constants range between 10  $\mu$ s and 50 ms [9]. The absorbance change associated with the middle of the three modes is opposite to those of the faster and slower ones. It is important to note that arsenazo III is of only limited applicability for the indication of rapid changes in Ca<sup>2+</sup> concentration. Usually, only those changes are readily analyzable which are about 5 times slower than the intrinsic relaxation modes of the indicator system; the limits of the time range are dependent on the indicator concentration. For example, a simple kinetic analysis of, e.g., a protein–Ca<sup>2+</sup> interaction indicated by arsenazo III, is restricted to the time range  $>50$  ms at  $[\text{Ar}_T] = 10^{-4}$  M and  $>0.3$  s at  $[\text{Ar}_T] = 5 \times 10^{-6}$  M.

Monovalent alkali metal ions like  $\text{Na}^+$  and  $\text{K}^+$  also form complexes with arsenazo III. It is found that  $\text{Na}^+$ –arsenazo III complexes contribute significantly to the absorbance at 602 nm; the equilibrium constant of the  $\text{Na}^+$ –Ar complexes is estimated to be 0.1 M at zero ionic strength, pH 7.0 and 293 K [9]. Hence, monovalent alkali metal ions interact specifically with arsenazo III and compete with  $\text{Ca}^{2+}$  for the indicator molecule.

As the final point, it need be mentioned that we investigated possible contributions from other types of complexes, e.g.,  $\text{Ca}_2\text{Ar}_2$ ,  $\text{Ca}_3\text{Ar}_2$  and  $\text{Ca}_2\text{Ar}_3$ , but these were ruled out in the concentration ranges covered here, because the corresponding constancy criteria for equilibrium constants could not be satisfied. The interaction of arsenazo III with  $\text{Ca}^{2+}$  ions can be summarized by scheme (12):



### Acknowledgement

We thank Ute Santarius for her skillful and devoted technical assistance. The financial support of the Deutsche Forschungsgemeinschaft, grant Ne 227, is gratefully acknowledged.

### References

- [1] G. Weissman, T. Collins, A. Evers and P. Dunham. *Proc. Nat. Acad. Sci. U.S.A.* 73 (1976) 510.
- [2] W.C.K. Chiu and D.H. Haynes, *Biophys. J.* 18 (1977) 3.
- [3] R. DiPolo, J. Requena, F.J. Brinley, L.S. Mullins, A. Scarpa and T. Tiffert, *J. Gen. Physiol.* 67 (1976) 433.
- [4] V. Michaylova and P. Ilkova, *Anal. Chim. Acta* 53 (1971) 194.
- [5] A. Scarpa, F.J. Brinley and G. Dubyak, *Biochem.* 17 (1978) 1378.
- [6] S.T. Ohnishi, *Biochim. Biophys. Acta* 586 (1979) 217.
- [7] M.V. Thomas, *Biophys. J.* 25 (1979) 541.
- [8] N.C. Kendrick, *Anal. Biochem.* 76 (1976) 487.
- [9] H. Gottheiner, Ph.D. Thesis, University of Munich (1980).
- [10] P.L. Dorogi and E. Neumann, *Biophys. Chem.* 13 (1981) 117.